



# Deep ruptures around the hypocenter of the 12 May 2008 Wenchuan earthquake deduced from aftershock observations

Meijian An\*, Mei Feng, Changxing Long

*Institute of Geomechanics, Chinese Academy of Geological Sciences, Minzu Daxue Nanlu 11, Beijing 100081, China*

## ARTICLE INFO

### Article history:

Received 6 February 2009

Received in revised form 14 December 2009

Accepted 29 December 2009

Available online 11 January 2010

### Keyword:

Wenchuan earthquake

Aftershock

Rupture

Relative relocation

## ABSTRACT

On 12 May 2008, a great earthquake of Mw 7.9 occurred in Wenchuan, China. To record its aftershocks and investigate the distribution of deep ruptures associated with the event, we deployed a temporary short-period seismic network around the epicenter soon after the earthquake had occurred. A total of 6036 aftershocks were located from 108 days of seismic data with a high signal-to-noise ratio, collected from July to October 2008. These aftershocks were further processed using a double-differential location method, and 2878 aftershocks were retained in the relocated clusters. According to the distribution of aftershocks, we refined the location of the main shock hypocenter to 31.001°N, 103.280°E, 17 km deep. The spatial distribution of aftershocks reveals interesting features of the deep ruptures: (1) most aftershocks are located in the upper crust at depths shallower than 20 km, beneath surface outcrop of the Pengguan massif, indicating that the upper crust is brittle and seismogenic and that the brittle–ductile transition is located at the transition between the middle and upper crust; (2) a NW–SE-striking low-seismicity zone crossing through Yingxiu Town divides the study area into two blocks with contrasting distributions of deep seismicity, suggesting different rupture characteristics either side of the line; and (3) upward extrapolation of aftershock clusters intersects with the southern and northern arms of the Zipingpu Reservoir, indicating that aftershocks and future seismicity along the ruptures around the reservoir that were activated by the Wenchuan earthquake will be influenced by reservoir impoundment/drainage for several decades to come.

© 2010 Elsevier B.V. All rights reserved.

## 1. Introduction

On 12 May 2008, a great earthquake of magnitude Mw 7.9 occurred in Wenchuan County of Sichuan Province, western China. The earthquake and its strong aftershocks activated the ~300-km-long Longmen Shan fault system that marks the transition between mountains of the Tibetan Plateau and the Sichuan Basin (Fig. 1). It is thought that the earthquake occurred as a result of long-term uplift and eastward extrusion of the Tibetan Plateau (Burchfiel et al., 2008).

Fig. 2 shows the geography and tectonic setting of the study area. The active Longmen Shan fault system comprises the NE–SW-striking Wenchuan–Maoxian Fault in the northwest, the Yingxiu–Beichuan Fault in the central portion, and the Guanxian–Anxian fault in the southeast (blue lines in Fig. 2) (State Expert Committee of the Wenchuan Earthquake, 2008). The area between the Wenchuan–Maoxian and Yingxiu–Beichuan faults consists of diorites and granites of the Proterozoic Pengguan igneous massif; other areas are largely covered by sedimentary rocks. The Zipingpu Reservoir (demarcated by the 850 m topographic contour in Fig. 2) is located close (within

~15 km) to the epicenter of the Wenchuan earthquake, as taken from the MHDF (Monthly Hypocenter Data File) catalog. The reservoir is one of the largest along the Minjiang River, with a 159-m-high dam and a maximum capacity of  $1.112 \times 10^9 \text{ m}^3$ . The epicenter of the Wenchuan earthquake is located at the southern tip of the Pengguan massif, close to the junction between the Wenchuan–Maoxian and Yingxiu–Beichuan faults (Fig. 2).

Soon after the Wenchuan earthquake, many Chinese geologists carried out field investigations of the surface ruptures and co-seismic deformation (Chen et al., 2008; Dong et al., 2008; Ma et al., 2008). These studies reported that the main shock rupture around the epicenter is a NE–SW-striking, NW-dipping reverse fault with a minor right-slip component, consistent with the focal mechanism of the main shock (Fig. 1). The movement direction of the hanging wall of the Yingxiu–Beichuan Fault is shown by the yellow arrow in Fig. 2. However, because of the occurrence of strong seismic-related surface ruptures and landslides in the rugged mountains along the faults, field investigations were limited to scattered sites and no information was obtained on the nature of deep ruptures. The large distances between most operational seismic stations and the main shock (Huang et al., 2008; Liu et al., 2008; Zhu et al., 2008) means that the hypocentral resolution is inadequate for determining the rupture details around the hypocenter of the main shock. For example, the main shock hypocenter in the Chinese Seismological Network (CSN) catalog

\* Corresponding author. Tel.: +86 10 68484113; fax: +86 10 68422326.

E-mail addresses: [meijianan@yahoo.com.cn](mailto:meijianan@yahoo.com.cn) (M. An), [mei\\_feng\\_cn@yahoo.com.cn](mailto:mei_feng_cn@yahoo.com.cn) (M. Feng), [cxlong@hotmail.com](mailto:cxlong@hotmail.com) (C. Long).

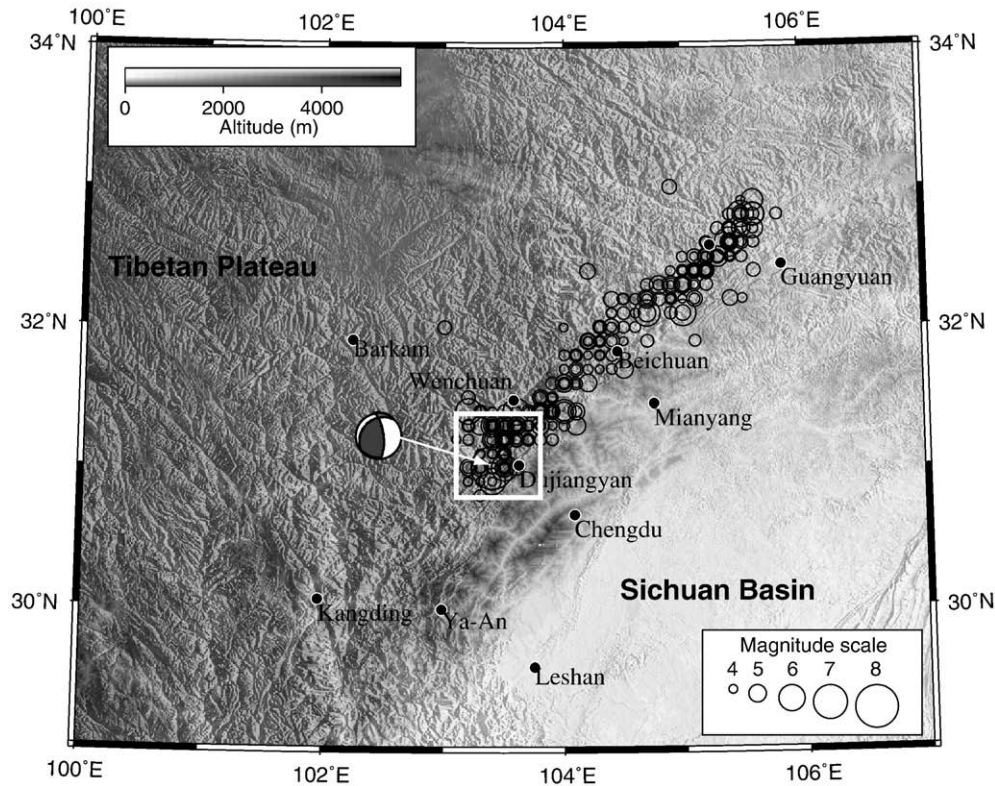


**Fig. 1.** Location of the study area (white rectangle) and geography of the surrounding area. The 2008 Wenchuan earthquake and strong aftershocks ( $M_s \geq 4$ ) that occurred before 28 January 2009 are shown as black open circles. Epicentral information for the aftershocks was obtained from the CSN catalog ([www.csndmc.ac.cn](http://www.csndmc.ac.cn)). The focal mechanism of the main shock is from [www.globalcmt.org](http://www.globalcmt.org).

(31.0°N, 103.4°E, 14 km deep) is different to that in the NEIC (National Earthquake Information Center) MHDF (Monthly Hypocenter Data File) catalog (31.002°N, 103.322°E, 19 km). The hypocenter uncertainty in these catalogs is greater than ~5 km, which is inadequate to obtain precise information regarding the rupture plane of the main shock.

Because aftershocks following a strong main shock generally occur in large numbers and can help to delineate the rupture upon which the main shock occurred, we deployed a temporary short-period seismic network around the main shock epicenter at the end of June 2008, with an average station spacing <10 km. The aim of this initiative was to gain a better understanding of the earthquake process and to investigate the features of deep rupture beneath the surface based on precise aftershock observations. The aftershocks recorded by this local seismic network were then analyzed to determine the earthquake rupture planes.

## 2. Data and methods

The temporary seismic network established around the main shock epicenter was constructed in two stages. The first 16 portable seismic stations (red triangles in Fig. 2) were installed at the end of June 2008; the other 7 stations (pink triangles in Fig. 2) were installed in September 2008. Because of difficulties related to road access, the seismic stations are not evenly distributed throughout the study area. All the seismic stations are equipped with short-period Mark Products (Sercel) L-22D sensors. The L-22D sensor has a standard frequency of 2 Hz and a flat frequency response at frequencies of >4 Hz.

Only those events simultaneously recorded by at least 10 stations with high signal-to-noise ratio were selected for analysis. The hypocentral locations were preliminarily determined using the program HYPO71 (Lee and Lahr, 1972). A 1-D six-layer velocity model (Zhao et al., 1997) for the Longmen Shan fault system was used

to locate aftershocks. To test the robustness of the hypocenter determination method, we also determined the hypocenters of aftershocks using the program HYPOELLIPSE (Lahr, 1999), which takes into account station altitude; the two programs produced similar distributions of hypocenters. Local magnitude (ML) was computed using the formula and constants provided by Richter (1958); however, the computed magnitude may be underestimated because we used high-frequency sensors. We processed 108 days of seismic data (from 6 July 2008) and retrieved 6036 aftershocks, among which 1565 have a local magnitude greater than 2.0.

To improve the precision of the hypocenter determination, we relocated the earthquakes using the relative location method HYPODD (Waldhauser and Ellsworth, 2000). Cross-correlation differential times of close aftershocks recorded by a given station provide useful constraints in reducing the uncertainties involved in determining relative earthquake locations by HYPODD. However, the primary assumption that guarantees the usefulness of the cross-correlation differential times is that the hypocenters are closely spaced such that the observed waveforms of two close earthquakes are similar due to the similarity in Green's functions, which characterize the source-receiver paths. The close earthquakes may represent repeated slip of the same patch on a fault (Baisch et al., 2008).

In processing the data, the focal mechanisms of close aftershocks were commonly found to differ from each other. Fig. 3 shows that the vertical component waveforms of two neighboring aftershocks recorded by a given station are somewhat different, indicating that the focal mechanisms could also be very different. The contrasting focal mechanisms could reflect earthquakes from different secondary ruptures with different properties or the complex evolution of stress redistribution occurring via the shocks, as aftershocks are a consequence of stress redistribution related to the main shock. Such aftershocks occur as failures upon smaller fault asperities (Strehlau,

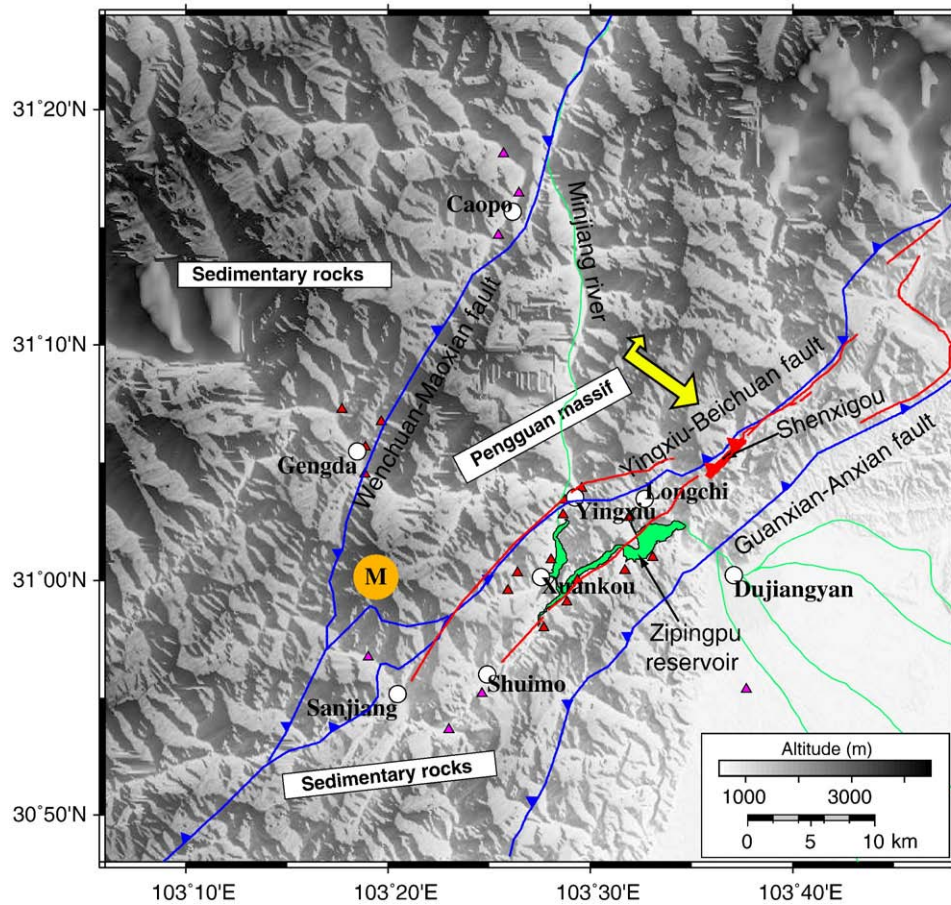


**Fig. 2.** Geography and tectonic setting of the study area, with topography shown by shading (topography data are SRTM-30 from USGS). Triangles are seismic stations, with red triangles indicating stations deployed at the end of June 2008, and pink triangles indicating stations deployed in September 2008; yellow circle is the hypocenter of the main shock from the MHDF catalog. Blue lines are the Longmen Shan faults; green lines are rivers, and green areas represent the Zipingpu Reservoir. Red lines indicate co-seismic surface ruptures (Xu et al., 2009). The thick red segment labeled as Shenxigou denotes the escarpment along the Yingxiu-Beichuan Fault, which was formed by the main shock (Chen et al., 2008; Dong et al., 2008; Xu et al., 2008). The thick yellow arrow indicates the movement direction of the hanging wall of the Yingxiu-Beichuan Fault.

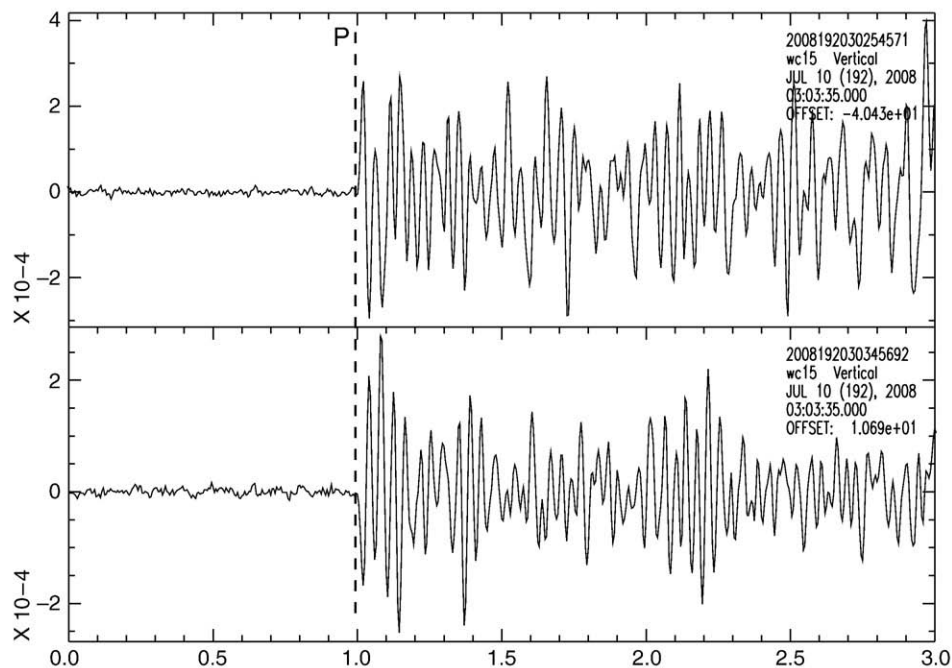


**Fig. 3.** Vertical-component waveforms of two neighboring aftershocks recorded by a single seismic station. The hypocenters of the two aftershocks, as determined by HYP071, are located at (31.002°N, 103.404°E, 6.15 km deep) and (31.000°N, 103.403°E, 6.00 km deep), respectively.

1986) with potentially different focal mechanisms to that of the main shock. Such a scenario requires event selection via waveform cross-correlation analysis, which is time-consuming because thousands of aftershocks were observed in the present study; consequently, we did not carry out waveform cross-correlation analysis when relocating aftershocks by HYPODD.

Travel time differences obtained from manually picked P- and S-wave arrival times were used in HYPODD. We selected 3007 high-quality aftershocks (clear P or S phases and simultaneously recorded by at least 15 stations) from the 6036 preliminary located events for further processing by HYPODD, among which there were 1093 events with  $ML > 2.0$ . The number of events relocated by HYPODD is less than the number of input events, and depends on the parameter configuration in the relocation process. We used eight iterations for the conjugate gradient method in the HYPODD inversion technique (Waldhauser and Ellsworth, 2000). A maximum of eight neighboring events were considered to be linked to each other for relocation in HYPODD. Because picking of the S phase involves a larger uncertainty than that for the P phase, we selected the *a priori* weights (1:0.5) assigned for P- and S-wave travel times based on our tests and previous studies (e.g., Mandal and Horton, 2007). The average relative uncertainties for the aftershocks upon relocation can be several hundreds of meters in both epicentral location and focal depth for a network of stations spaced at intervals of ~10–30 km (Mandal and Horton, 2007).

Previous studies on aftershocks of the Wenchuan earthquake using regional network observations reported a location uncertainty of ~1 km in the horizontal and ~2.5 km in the vertical (Zhu et al., 2008; Huang et al., 2008; Chen et al., 2009). In our case, the average distance between stations was <~10 km, less than those in the above studies; consequently, the relative uncertainty in hypocenter locations is expected to be much smaller than that reported previously. The absolute uncertainties for aftershock locations are difficult to estimate because of the structural complexity of the study area. Considering that the structure is highly complex, and based on the results of previous studies, we propose a location uncertainty of <~1 km in the horizontal and <~2.5 km in the vertical. Finally, relocated aftershock clusters obtained from HYPODD include 2878 events from the 3007 aftershocks. Because the hypocenters of the relocated aftershocks have a higher resolution than those determined by HYPO71, only the relocated hypocenters are discussed below.

We deployed an additional seven stations at the end of September 2008, with superior station coverage compared with the first-stage deployment; consequently, the location resolution for aftershocks recorded from October 2008 is expected to be better than that for aftershocks recorded prior to this date. However, the monthly patterns of aftershock clusters show no clear difference between July and October 2008. Accordingly, the change in station distribution is not considered to influence our discussion based on the results presented below.

### 3. Results

The epicenters of the 6036 preliminary located events (by HYPO71) and 2878 relocated aftershocks (by HYPODD) are shown in Fig. 4a and b, respectively. Fig. 4 shows that the main shock, located at the southwestern end of the Pengguan massif, and the aftershock epicenters are distributed mainly in the hanging wall of the Yingxiu–Beichuan Fault. The southern end of the active zone along the Longmen Shan fault system (see Fig. 1) should be located southwest of the aftershock clusters (Fig. 4b) in the vicinity of the location of the main shock, and it also lies near the intersection of the Wenchuan–Maoxian and Yingxiu–Beichuan faults. The epicenters in the study area appear to be separated into two clusters by a NW–SE-striking line (thick dashes marked as “L1” in Fig. 4a) that crosses Yingxiu Town and Zipingpu Reservoir. The pattern of seismicity differs either side of this line; a similar feature is

apparent in the distribution of strong aftershocks ( $M_s > 4$ ; Fig. 1). Relatively minor seismicity is observed along the line itself. The Yingxiu–Beichuan Fault shows an abrupt change in strike near Yingxiu Town. These observations may indicate that line L1 is a regional tectonic boundary that oriented at a high angle to the Longmen Shan fault belt. Because the line runs along a NW–SE-oriented valley from Dujiangyan to Yingxiu and Gengda (see Figs. 2 and 4), it is referred to as the Dujiangyan–Yingxiu–Gengda tectonic line.

Fig. 5 shows the distribution of aftershocks along three cross-sections. The aftershock distribution depends on the projection distance ( $d$ ); that is, aftershocks located within a belt bounded by surfaces within  $\pm d$  of and parallel to the central line are considered representative and are projected onto the line of the cross-section. For comparison, we show aftershocks using projection distances of 3.5 and 7.0 km. The aftershock distribution on cross-sections with a projection distance of 3.5 km (upper panels in Fig. 5) is similar to that on cross-sections with a projection distance of 7.0 km (lower panels in Fig. 5); consequently, the subsequent discussion is based on the latter cross-sections.

The depths of relocated aftershocks generally extend down to ~20 km, with few events located at depths less than 5 km (Fig. 5). Given that the cutoff depth of ~20 km represents the base of the upper crust along the Longmen Shan fault system (Zhao et al., 1997; Bassin et al., 2000), the seismicity distribution indicates that the upper crust in the study area is brittle and seismogenic, and that the brittle–ductile transition occurs at the transition between the middle and upper crust. Since most of the aftershocks are found beneath surface outcrops of the Pengguan massif, the shallow area with sparse aftershocks may represent the base of this strong igneous body. The scarcity of relocated aftershocks at shallow depth could reflect our selection criterion regarding a minimum of 15 usable P phases, as shallow aftershocks are of smaller magnitude and were recorded by few stations.

Cross-section a–a’ is oriented NW–SE and crosses the southern part of the study area, south of the Dujiangyan–Yingxiu–Gengda tectonic line (Fig. 4b), at a high angle to the Longmen Shan fault system. The aftershocks depicted on this cross-section (Fig. 5a) show a convergence at depths down to ~20 km. The cluster center plane, marked by P2 in Fig. 5a, is characterized by a dip of ~45°, and its extrapolation to the surface is located around the main shock surface rupture in the valley between Xuankou Town and Shuimo Town, the southwestern arm of the Zipingpu Reservoir and ~10 km to the reservoir dam; therefore, P2 is considered to represent the deep rupture associated with the main shock. Fig. 5a also shows that the footwall of the Yingxiu–Beichuan Fault is active and that part of the Guanxian–Anxian Fault (F1 in Fig. 5a) may have been activated by the Wenchuan earthquake.

The western cluster boundary, plane P1, is near-vertical and located east of the Wenchuan–Maoxian Fault (F3 in Fig. 5a). P3, where located just above the main shock hypocenter (from MHDF), is the centerline of a linear aftershock cluster, possibly a secondary rupture. The above cluster distribution suggests that the regional upper crust is so inhomogeneous and complex that earthquake rupture is insufficiently described based solely on three active faults of the Longmen Shan fault system. Basically, all aftershocks are distributed around the middle plane (P2) and the Yingxiu–Beichuan Fault, which confirms that this fault was ruptured during the Wenchuan earthquake, as reported by earlier field investigations (Chen et al., 2008; Dong et al., 2008; Ma et al., 2008).

According to the main shock focal mechanism and the results of field investigations, the western hanging wall of the main shock rupture (the Yingxiu–Beichuan Fault) was thrust to the east. Considering the above results, the thrust event not only caused brittle fractures in the footwall of the Yingxiu–Beichuan Fault, but also in the hanging wall above the main shock hypocenter and close to the Wenchuan–Maoxian Fault.

Cross-section b–b' is oriented NW–SE across the northern part of the study area, north of the Dujiangyan–Yingxiu–Gengda tectonic line (Fig. 4b). The section is oriented perpendicular to the Longmen Shan fault system. The aftershocks depicted in this cross-section (Fig. 5b) show a different rupture feature to that in cross-section a–a'. In section b–b', the relocated hypocenters delineate a distinct NW-dipping belt of seismicity down to 20 km depth (bounded by dashes in the figure). Upward extrapolation of the central line of the seismic belt (solid line in the figure) intersects with the Shenxigou escarpment along the Yingxiu–Beichuan Fault (Fig. 2), close to Longchi Town and the northern arm of the Zipingpu Reservoir. The escarpment formed during thrusting along the Yingxiu–Beichuan Fault during the great Wenchuan earthquake (Chen et al., 2008; Dong et al., 2008; Xu et al., 2008). The rupture in this cross-section dips to the northwest at a slightly smaller angle than that of P2 in section a–a'.

Cross-section 1–1' is oriented SW–NE across the Pengguan massif in the hanging wall of the Yingxiu–Beichuan Fault, approximately parallel to the Longmen Shan fault system (Fig. 4b). The section reveals that aftershocks located southwest of Yingxiu are concentrated within a belt that dips to the SW at  $\sim 45^\circ$  (Fig. 5c). Upward extrapolation of the central line of the belt intersects with Yingxiu Town, more or less corresponding to the position of the Dujiangyan–Yingxiu–Gengda tectonic line in Fig. 4a, possibly indicating that the

line is the surface expression of a fault. This tentatively identified fault is termed the Dujiangyan–Yingxiu–Gengda Fault. Given that aftershocks are concentrated along the Longmen Shan fault system in the area northeast of the main shock, the area south of the hypocenter of the Wenchuan earthquake appears not to have been activated; consequently, the hanging wall of the potential fault may have remained unmoved during the great earthquake.

In the case that the hanging wall of the Yingxiu–Beichuan Fault was thrust to the east (thick yellow arrow in Fig. 4a), the footwall of the potential fault (the Dujiangyan–Yingxiu–Gengda Fault) should record displacement to the east, making it a strike-slip fault. Furthermore, because the main shock rupture along the Yingxiu–Beichuan Fault involved a minor right-slip component, the hanging wall of the Yingxiu–Beichuan Fault, located northeast of the hypocenter, should record a minor component of movement to the northeast (thin yellow arrow in Fig. 4a), indicating that the hanging wall of the potential fault records a minor normal-fault component. Interestingly, the area of Yingxiu Town itself shows less aftershock activity than do neighboring areas to the northeast and southwest. To the northeast of Yingxiu Town, aftershocks define a belt that dips to the NE at  $\sim 30^\circ$ ; therefore, the town separates two contrasting seismogenic zones. In summary, cross-section 1–1' reveals the lateral heterogeneity of the aftershock distribution and along-strike seismic

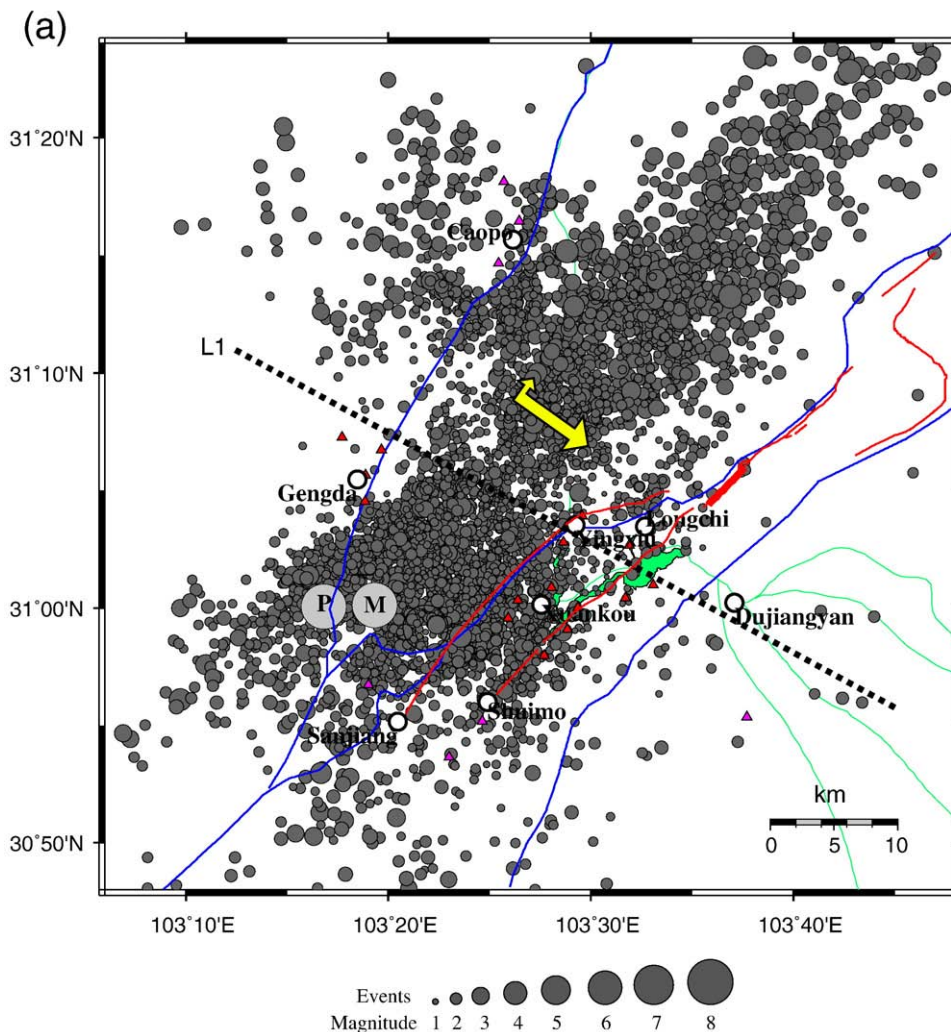


**Fig. 4.** Distribution of all 6036 aftershocks determined using HYPO71 (a) and the relocated aftershocks determined using HYPODD (b). The hypocenter of the main shock is shown as gray solid circles, with the hypocenter marked M being from the MHDF catalog, and that marked P is discussed in the text. Aftershocks are presented as dark-gray solid circles with radii proportional to seismic magnitude. The solid lines labeled 1–1', a–a', and b–b' indicate the central lines of the cross-sections shown in Fig. 5, and dashed rectangles mark the 7-km-wide zones projected onto the cross-sections. The tectonic and geographical boundaries are the same as in Fig. 2.

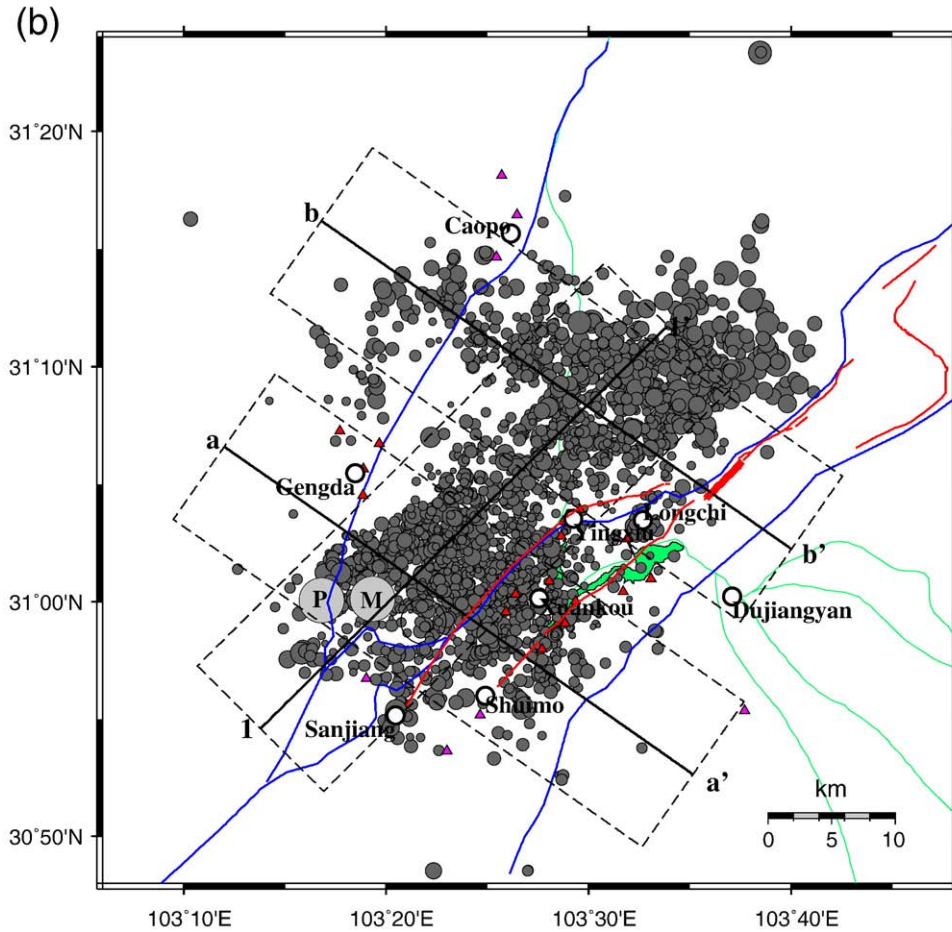


Fig. 4 (continued).

activity in upper crust within the hanging wall of the Yingxiu–Beichuan Fault.

Combining cross-sections a–a' and 1–1', it is apparent that the strong Wenchuan earthquake was initiated in the crossing region of the SW-dipping (cross-section 1–1') and NW-dipping aftershock belts (cross-section a–a'). If the two belts represent the deep rupture of the Yingxiu–Beichuan Fault and a potential fault along the boundary line L1, respectively, then it is possible that the Wenchuan earthquake was initiated at the intersection region of the two faults. This feature is consistent with the proposal that the areas of initiation and cessation of a rupture always occur in an intersection region (King, 1986; Talwani, 1999).

Aftershocks are generated as a consequence of stress redistribution related to the main shock, occurring as failure along smaller fault asperities. Aftershocks involve lower stress values than the main shock and thus may occur at greater depths and over wider areas than the main shock (Strehlau, 1986). Consequently, the main shock rupture should be located inside the aftershock belts and at slightly shallower depths than the lower termination of aftershock clusters, as demonstrated by the spatial relationship between the main shock and aftershocks related to the 1989 Loma Prieta earthquake (figure 20H in Dietz and Ellsworth, 1997). However, the hypocenter of the Wenchuan earthquake, as documented in public catalogs (e.g., MHDF), is located outside of the aftershock cluster belt (see cross-sections a–a' and 1–1' in Fig. 5). According to the three-dimensional aftershock distribution, we propose that the main shock hypocenter was located at 31.001°N, 103.280°E, 17 km (marked as P in Figs. 4 and 5), ~4 km west of the MHDF hypocenter (marked as M).

The Wenchuan earthquake rupture process at shallow crustal depths was clearly not a simple frictional slip failure on the pre-existing, weak Longmen Shan fault system, but a more complex process that involved the fracturing of relatively strong rock. Moreover, local strong areas (asperities) that are highly resistant to rupture growth on a fault play a more important role in determining the size of an earthquake than does the rest of the fault plane, which has little resistance to rupture growth (Ohnaka and Kato, 2007). In the present case, because most of the aftershocks occurred beneath surface outcrop of the Pengguan massif, the portion of the upper crust that consists of the igneous massif may contain asperities that have inhibited the northeastward movement of the hanging wall of the Yingxiu–Beichuan Fault in recent centuries, although they were unlocked during the great Wenchuan earthquake. This may explain why the Wenchuan earthquake was initiated close to Yingxiu Town in the southwestern part of the Pengguan massif.

#### 4. Discussion

The active Longmen Shan fault system occurs along the steep margin between the Qinghai–Tibetan Plateau and the strong cratonic rocks of the Sichuan Basin. The main shock of the Wenchuan earthquake and related aftershocks occurred mainly along the NE–SW-striking Yingxiu–Beichuan Fault, which is one of the active Longmen Shan faults. It is widely accepted that this earthquake resulted from the accumulation of large amounts of stress due to tectonic interaction between the Tibetan Plateau and the Sichuan Basin (Burchfiel et al., 2008; Dong et al., 2008; Royden et al., 2008).

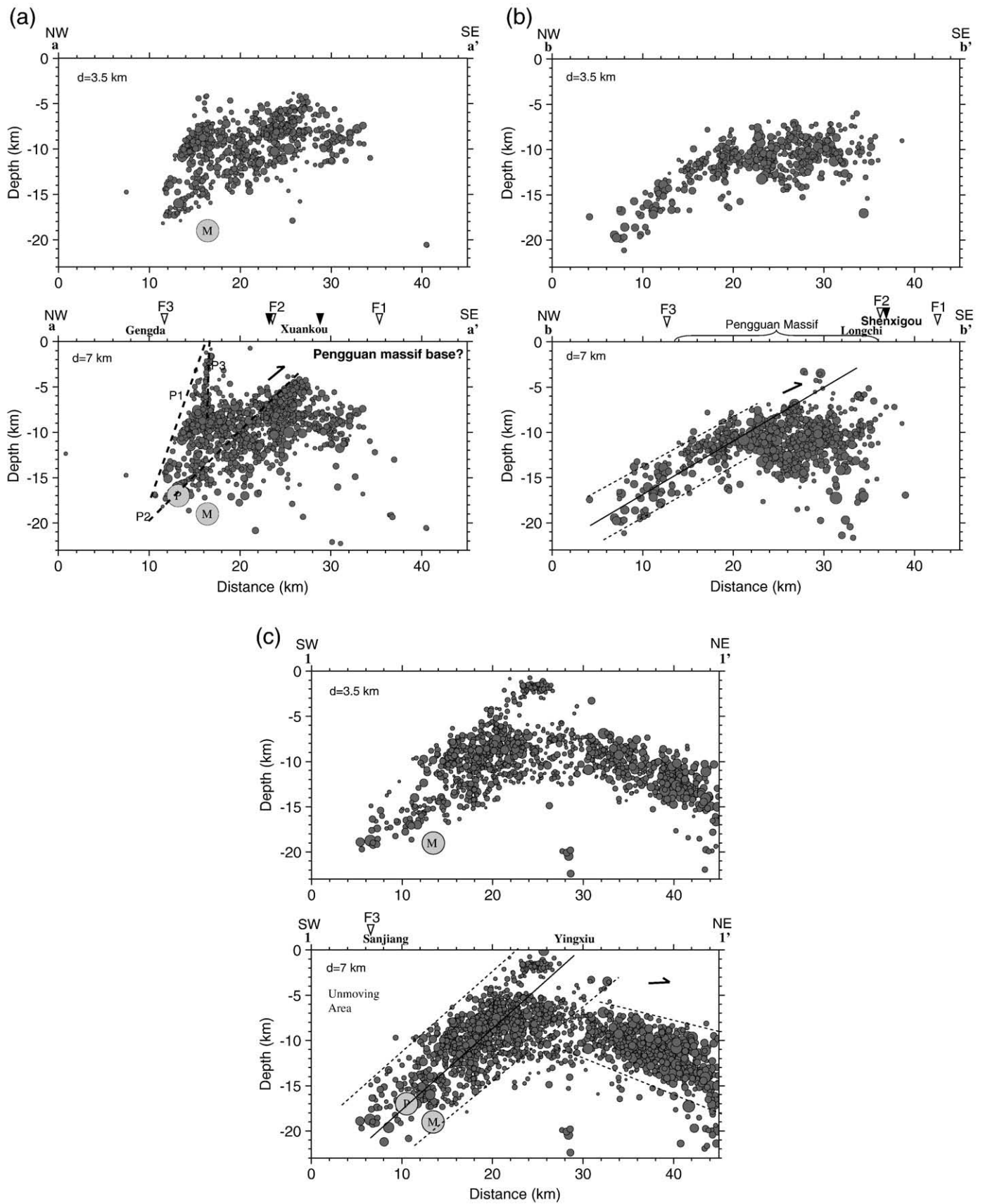


**Fig. 5.** Distribution of aftershocks along three vertical cross-sections, with projected distances ( $d$ ) of 3.5 km (upper panels) and 7.0 km (lower). Aftershocks within the area bounded by  $\pm d$  from the central line of the cross-section are projected onto the plane of the cross-section. The locations of the cross-sections and the areas within the projected distance of 7 km are shown in Fig. 4b. The filled inverted triangles indicate the positions of surface ruptures, and the hollow inverted triangles indicate the positions of three faults within the Longmen Shan fault system (F1 is the Anxian–Guanxian Fault, F2 is the Yingxiu–Beichuan Fault, and F3 is the Wenchuan–Maoxian Fault). Other symbols and labels are the same as in Fig. 4.

The present results show that the rupture belts around the epicenter are more complex than a simple NE–SW-striking, NW-dipping reverse fault with a minor right-slip component, as reported in earlier field-based studies. Furthermore, the locations of aftershock belts show a relation to the location of the Zipingpu Reservoir.

Regardless of whether the Wenchuan earthquake was related to the Zipingpu Reservoir, fault activity around the reservoir, as activated by the great Wenchuan earthquake, might have resulted in hydraulic connectivity between the reservoir and regional ruptures, or at least weakened the regional upper crust. Assuming hydraulic connectivity, seismicity in the region (within ~20 km of the reservoir) may be related to the reservoir for the next ~32 years, based on a hydraulic diffusivity of 0.1 m<sup>2</sup>/s and using the equation proposed by Talwani et al. (2007). Thus, the aftershocks and future seismicity along the ruptures around the reservoir that were activated by the Wenchuan earthquake may be influenced by the reservoir impoundment and drainage for several decades to come.

During the Wenchuan earthquake, most of the accumulated stress would have been released; therefore, a stronger earthquake is unlikely to occur in this region for a long time to come. Furthermore, if the ruptures around the reservoir activated by the Wenchuan earthquake resulted in hydraulic connectivity between the reservoir and regional faults, the Pengguan massif would be more susceptible to failure than before. Consequently, the regional upper crust of the Pengguan massif will be unable to accumulate as large a magnitude of stress as that released during the Wenchuan earthquake; that is, it is highly unlikely that an earthquake with a comparable magnitude to that of the Wenchuan earthquake will occur in the Pengguan massif in the near future.

## 5. Conclusion

To record the aftershocks following the Mw 7.9 Wenchuan earthquake of 12 May 2008 and to investigate its deep rupture distribution, we deployed 23 short-period seismic stations around the main shock epicenter soon after the earthquake occurred. By processing 108 days of high-quality seismic data, we located 6036 aftershocks using HYPO71 and refined them as 2878 clustered aftershocks using HYPODD. Most aftershocks occurred at depths of less than 20 km beneath surface outcrop of the Pengguan massif, indicating that the upper crust in the study area is brittle and seismogenic, and that the brittle–ductile transition is located at the transition between the middle and upper crust. The aftershocks in the southwestern and northeastern parts of the study area show contrasting horizontal and vertical distributions, separated by a NW–SE-striking belt with low seismicity, possibly corresponding to a regional tectonic boundary or a potential fault.

The aftershocks were mainly concentrated along the hanging wall of the NE–SW-striking Yingxiu–Beichuan Fault, confirming that the Wenchuan earthquake initiated along this fault. The aftershocks around the main shock epicenter delineate two ruptures: one dipping to the SW and another to the NW, suggesting that the great Wenchuan earthquake was initiated at the crossing region between two faults with contrasting dips.

Assuming that the main shock rupture was located inside the aftershock belts and slightly shallower than the lowermost extent of the aftershock clusters, we propose that the main shock hypocenter was located at 31.001°N, 103.280°E, 17 km deep, which is ~4 km west of the hypocenter in the MHDF catalog.

The upward extrapolation of the aftershock belts around the main shock epicenter intersects with the arms of the Zipingpu Reservoir. Regardless of whether the Wenchuan earthquake was related to the reservoir, the aftershocks and future seismicity along the ruptures around the reservoir that were activated by the Wenchuan earthquake may be influenced by the reservoir impoundment and drainage for decades to come. Furthermore, if the ruptures around the reservoir

that were activated by the strong Wenchuan earthquake have resulted in hydraulic connectivity within the Pengguan massif, there would be little or no chance of future earthquakes with a magnitude comparable to that of the Wenchuan earthquake.

## Acknowledgements

Because this study was initiated at short notice, we received timely support from the Ministry of Land and Resources of China (MLR), Chinese Academy of Geological Sciences (CAGS; especially from the administration team at the Institute of Geomechanics), Chengdu Institute of Geology and Mineral Resources, and local governments. We thank Changhong He, Jizhong Zhang, Huijun Li, Taoyuan Fan, and Jinhai Zhu (Institute of Geomechanics) for their help in deploying seismic stations.

Financial support was provided by Basic Research Foundation of the Institute of Geomechanics (CAGS; grant DZLXJK200707) and the NSFC (grant 40674058). We are grateful to Prof. Marcelo S. Assumpção, Yue Zhao, and two anonymous reviewers for their constructive comments and suggestions that significantly improved the quality of the manuscript. The figures in this article were produced using the Generic Mapping Tool (Wessel and Smith, 1991).

## References

- Baisch, S., Ceranna, L., Harjes, H.-P., 2008. Earthquake cluster: what can we learn from waveform similarity? *Bull. Seismol. Soc. Am.* 98 (6), 2806–2814.
- Bassin, C., Laske, G., Masters, G., 2000. The current limits of resolution for surface wave tomography in North America. *EOS Trans. AGU* 81, F897.
- Burchfiel, B.C., et al., 2008. A geological and geophysical context for the Wenchuan earthquake of 12 May 2008, Sichuan, People's Republic of China. *GSA Today* 18 (7), 4–11.
- Chen, G.-H., et al., 2008. Quantitative analysis of the co-seismic surface rupture of the 2008 Wenchuan earthquake, Sichuan, China along the Beichuan–Yingxiu fault. *Seismol. Geol.* 30 (3), 723–737.
- Chen, J.-H., et al., 2009. Seismotectonic study by relocation of the Wenchuan MS 8.0 earthquake sequence. *Chinese J. Geophys.* 52 (2), 390–397.
- Dietz, L.D., Ellsworth, W.L., 1997. Aftershocks of the Loma Prieta earthquake and their tectonic implications. In: Reasenber, P.A. (Ed.), *The Loma Prieta, California, Earthquake of October 17, 1989 – Aftershocks and Postseismic Effects*, pp. 5–47.
- Dong, S., et al., 2008. Surface rupture investigation of the Wenchuan Ms 8.0 earthquake of May 12th, 2008, West Sichuan, and analysis of its occurrence setting. *Acta Geoscientia Sin.* 29 (3), 392–396.
- Huang, Y., Wu, J., Zhang, T., Zhang, D., 2008. Relocation of the M 8.0 Wenchuan earthquake and its aftershock sequence. *Sci. China Ser. D-Earth Sci.* 51 (12), 1703–1711.
- King, G.C.P., 1986. Speculations on the geometry of the initiation and termination processes of earthquake rupture and its relation to morphology and geological structure. *Pure Appl. Geophys.* 124 (3), 567–585.
- Lahr, J.C., 1999. HYPOELLIPSE: a computer program for determining local earthquake hypocentral parameters, magnitude, and first-motion pattern.
- Lee, W.H.K., Lahr, J.C., 1972. HYPO71: a computer program for determining hypocenter, magnitude, and first motion pattern of local earthquakes (U.S. Geol. Surv. Open-File Rep.).
- Liu, Q.-Y., et al., 2008. The Ms 8.0 Wenchuan earthquake: preliminary results from the Western Sichuan mobile seismic array observations. *Seismol. Geol.* 30 (3), 584–596.
- Ma, Y.-S., et al., 2008. Co-seismic deformation features and segmentation of the Ms 8.0 Wenchuan earthquake in Sichuan, China. *Geol. Bull. China* 27 (12), 2076–2085.
- Mandal, P., Horton, S., 2007. Relocation of aftershocks, focal mechanisms and stress inversion: Implications toward the seismo-tectonics of the causative fault zone of Mw7.6 2001 Bhuj earthquake (India). *Tectonophysics* 429 (1–2), 61–78.
- Ohnaka, M., Kato, A., 2007. Depth dependence of constitutive law parameters for shear failure of rock at local strong areas on faults in the seismogenic crust. *J. Geophys. Res.* 112, B07201.
- Richter, C.F., 1958. *Elementary Seismology*. W H Freeman & Co (Sd), San Francisco, California.
- Royden, L.H., Burchfiel, B.C., van der Hilst, R.D., 2008. The geological evolution of the Tibetan Plateau. *Science* 321 (5892), 1054–1058.
- State Expert Committee of the Wenchuan Earthquake, 2008. *Atlas of Earthquake and Geological Disasters for the Wenchuan Earthquake*. SinoMaps Press, Beijing.
- Strehlau, J., 1986. A discussion of the depth extent of rupture in large continental earthquakes. In: Das, S., Boatwright, J., Scholz, C.H. (Eds.), *Earthquake Source Mechanics*. American Geophysical Union, Washington, D.C., pp. 131–145.
- Talwani, P., 1999. Fault geometry and earthquakes in continental interiors. *Tectonophysics* 305 (1–3), 371–379.
- Talwani, P., Chen, L., Gahalaut, K., 2007. Seismogenic permeability, *ks*. *J. Geophys. Res.* 112, B07309.

- Waldhauser, F., Ellsworth, W.L., 2000. A double-difference earthquake location algorithm: method and application to the Northern Hayward Fault, California. *Bull. Seismol. Soc. Am.* 90 (6), 1353–1368.
- Wessel, P., Smith, W.H.F., 1991. Free software helps map and display data. *EOS Trans. AGU* 72, 411.
- Xu, Z., et al., 2008. Uplift of the Longmen Shan range and the Wenchuan earthquake. *Episodes* 31 (3), 291–301.
- Xu, X., Wen, X., Yu, G., Chen, G., Klinger, Y., 2009. Coseismic reverse- and oblique-slip surface faulting generated by the 2008 Mw 7.9 Wenchuan earthquake, China. *Geology* 37 (6), 515–518.
- Zhao, Z., Fan, J., Zheng, S.H., Hasegawa, A., Horiuchi, S., 1997. Crustal structure and accurate hypocenter determination along the Longmenshan fault zone. *Acta Seismol. Sin.* 10 (6), 761–768.
- Zhu, A.-L., et al., 2008. Relocation of the Ms 8.0 Wenchuan earthquake sequence in Part: Preliminary seismotectonic analysis. *Seismol. Geol.* 30 (3), 759–767.